

### 3차원 속도 토모그래피를 이용한 북한지역의 지각구조 연구

김소구<sup>1)</sup> · 신종우<sup>2)</sup>

<sup>1)</sup>한양대학교 지구해양학과, <sup>2)</sup>국립문화재연구소

## Study of Crustal Structure in North Korea Using 3D Velocity Tomography

So Gu Kim<sup>1)</sup> · Jong Woo Shin<sup>2)</sup>

<sup>1)</sup>Hanyang University, Dept. of Earth & Marine Sciences

<sup>2)</sup>National Research Institute of Cultural Properties

### 요 약

북한 지역 60km 하부 지각구조에 관한 새로운 결과를 토모그래피 방법으로 연구하였다. 한반도와 주변에서 얻어진 1013개의 P파와 S파 주행시간이 사용된다. 또한, 이 연구에서 토모그래피 알고리즘에 의해서 모든 지진의 진원이 재결정 된다. 속도구조의 파라미터화는 지진파 밀도에 따라 분포된 Node에 의해서 결정된다. 4개 Level의 120 Node가 각각 P파와 S파의 속도 구조에 적용된다. 연구 결과로 깊이 8Km의 량림 육괴의 깊이에서 P파와 S파 속도 이상변화는 각각 높고 낮게 나타났다. 그 반면에 평남분지의 P파와 S파 속도는 24Km 깊이까지 모두 낮게 나타났다. 그것은 량림 육괴는 지하수나 온천 등으로 포화 된 단층 및 파쇄대를 많이 갖고 있는 시생대-초기 하부 원생대 육괴로 되어 있고, 반면에 평남분지의 평양-사리원 일대는 상부 원생대, 실루리안, 상부 고생대와 하부 중생대 기원의 퇴적층으로 채워진 내부 플랫폼 폼 함몰로 되어 있음을 의미한다. 특히 백두산 하부 8, 16, 24Km 깊이에서 높은 P파와 S파의 속도 이상은 고결된 마그마 물체의 천부 도랑일지 모른다. 그러나 38Km에서 낮은 P파와 S파 속도 이상은 용융상태의 저속도 마그마방과 관련 된 것으로 본다. 우리는 또한 사리원을 포함한 용진 분지에서 Moho불연속면이 약 55Km임을 발견하였다. 백두산의 모호불연속면은 38Km가량 된다. 특히 백두산 Moho에서  $V_p/V_s$ 의 높은 비율은 지각과 맨틀 경계에서 용융물체가 있는 것으로 간주된다. 또한 본 연구는 또한 량림육괴 순상지(Shield)의 끝 가장자리인 묘향산 지역 하부 40Km에서 매우 높은 P파와 S파 속도 구조를 갖는 물체가 있음을 보여 주었다.

**주요어:** 지진 토모그래피, 해상도, 초동, 위상, 재결정

**ABSTRACT:** New results about the crustal structure down to a depth of 60 km beneath North Korea were obtained using the seismic tomography method. About 1013 P- and S-wave travel times from local earthquakes recorded by the Korean stations and the vicinity were used in the research. All earthquakes were relocated on the basis of an algorithm proposed in this study.

\* Corresponding author: sogukim@hanmail.net

Parameterization of the velocity structure is realized with a set of nodes distributed in the study volume according to the ray density. 120 nodes located at four depth levels were used to obtain the resulting P- and S-wave velocity structures.

As a result, it is found that P- and S-wave velocity anomalies of the Rangnim Massif at depth of 8 km are high and low, respectively, whereas those of the Pyongnam Basin are low up to 24 km. It indicates that the Rangnim Massif contains Archean-early Lower Proterozoic Massif foldings with many faults and fractures which may be saturated with underground water and/or hot springs. On the other hand, the Pyongyang-Sariwon in the Pyongnam Basin is an intraplate depression which was filled with sediments for the motion of the Upper Proterozoic, Silurian and Upper Paleozoic, and Lower Mesozoic origin. In particular, the high P- and S-wave velocity anomalies are observed at depth of 8, 16, and 24 km beneath Mt. Backdu, indicating that they may be the shallow conduits of the solidified magma bodies, while the low P- and S-wave velocity anomalies at depth of 38 km must be related with the magma chamber of low velocity bodies with partial melting. We also found the Moho discontinuities beneath the Ongin Basin including Sariwon to be about 55 km deep, whereas those of Mt. Backdu is found to be about 38 km. The high ratio of P-wave velocity/ S-wave velocity at Moho suggests that there must be a partial melting body near the boundary of the crust and mantle. Consequently we may well consider Mt. Backdu as a dormant volcano which is holding the intermediate magma chamber near the Moho discontinuity. This study also brought interesting and important findings that there exist some materials with very high P- and S-wave velocity anomalies at depth of about 40 km near Mt. Myohyang area at the edge of the Rangnim Massif shield.

**Key Words:** Seismic tomography, resolution, first arrival, phase, relocation

## Introduction

Information about the 3D structure of the crust is important for understanding the main mechanisms of the crustal dynamics. The joint analysis of P- and S-wave velocity heterogeneities makes it possible to estimate the nature of anomalies in the crust. At the same time, information about the 3D velocity structure helps to improve the accuracy of earthquake location without increasing the number of stations. Precise location of seismicity provides reliable information about the main seismotectonic blocks, nature, and mechanism of seismic activity. This information

can be used for estimation of seismic risk.

The Korean Peninsula is a relatively aseismic region, though it is located just near the border of a big Amurian block, Baikal- Korea Plate (Kim et al. 2003) which extends from the Baikal Rift Zone in the west, east to the islands of Japan and Sakhalin, and south to NE China and the Korean Peninsula. At the same time, the close position of Korea to the great collision blocks makes the problems of estimation of seismic risk very difficult (Kim and Song, 1999).

The crust of North Korea consists mostly of ancient blocks (Geology of Korea, 1993). The main structures are orientated diagonally from SW to NE (see Fig. 1). The geological map of

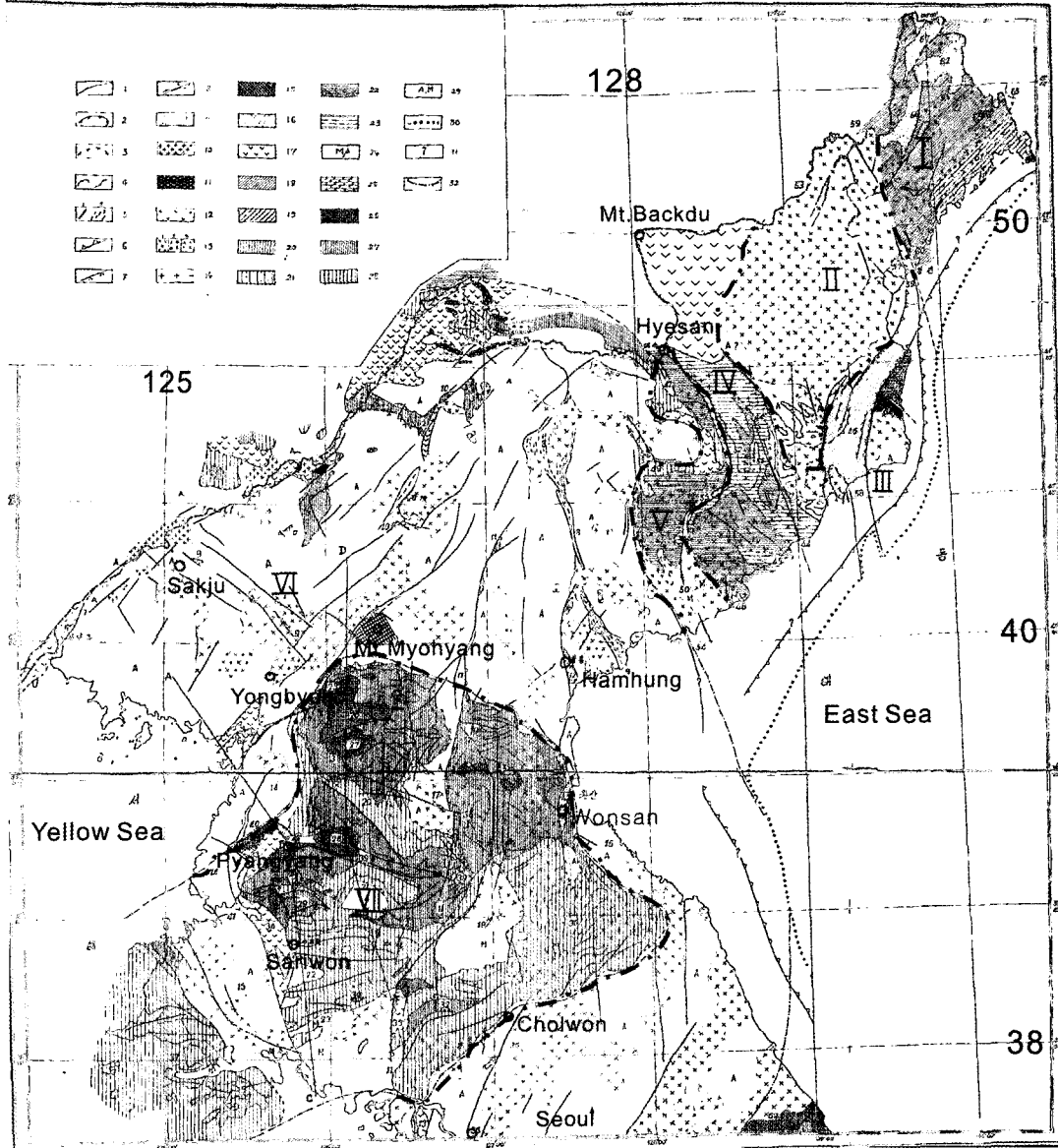


**Fig. 1.** Geological Map of North Korea  
 Reproduced from Ro Su Won (1964) and Geology of North Korea(1993)  
 I. Tumangang Fold Belt(Upper Paleozoic)  
 II. Kwanmo Massif(Archean-early Lower Proterozoic )  
 III. Kilju-Myongchon Basin (Cenozoic)  
 IV. Machollyong Massif(Late Lower-Proterozoic)  
 V. Hyesan-Riwon Sedimentary Basin  
 VI. Rangnim Massif(Archean-early Lower Proterozoic)  
 VII. Pyongnam Sedimentary Basin

North Korea is reproduced from Ro Su Won(Geological Structure and Underground Resources of NE Chosun and the maritime province south of Siberia, 1964. Tertiary and Quaternary basaltic flows cover in the western part.

Seismic velocity anomalies in the crust beneath Central and Southern Korea have been studied recently using the local tomography (Kim and Li, 1998a, Kim and Li, 1998b). Though, the present research has some important advantages as compared to the mentioned ones. This research is based on a significantly more advanced algorithm of tomographic inversion(Shin,2003). Also, the database used in this work is significantly larger. In this study we make separate analysis for P and S-waves that provides two independent models, while in the previous works they used only P-wave arrivals. We also made some tests to estimate the reliability of the obtained results.

### Seismic Data

In this work we used the travel times from 91 local earthquakes with a magnitude range from 2.5 to 5.5 recorded by Korean(North and South Korea) stations and stations from neighboring China and Russia ( see Fig. 2). In total 1013, we had 512 arrival times of P waves and 501 of S waves (including all phases of P and S waves). We did not consider in this research PmP and SmS, reflected from the Moho discontinuity, since they are mostly sensible to the Moho depth variation and not to the 3D velocity structure in the crust and furthermore we selected the first arrival times of P and S waves complying with Fermat's Principle. The number of P and S phases produced by one source and recorded by different stations is ranged from 10 to 40

(average value is 25). This is sufficient to locate accurately most of the events. All the stations and earthquakes used in this research are shown in Fig. 2. The ray paths used for inversion are depicted in this figure by light gray lines.

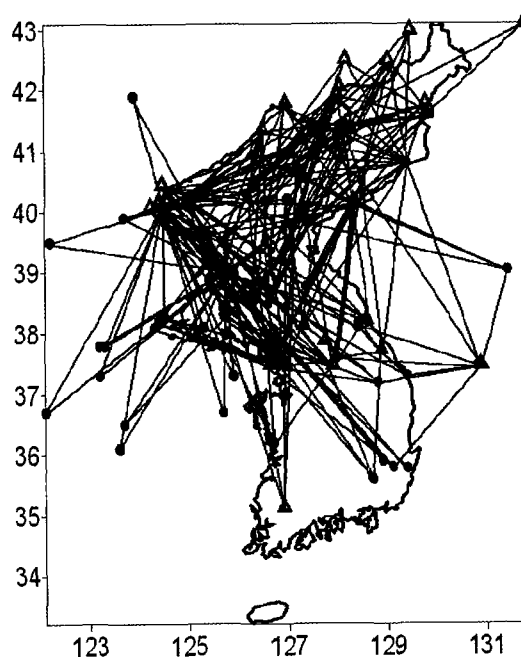


**Fig. 2.** Distribution of seismic stations(triangles) and local events(circles) used for inversion.

We used a simple one-dimensional continuous reference model. The velocities were set at certain depth levels. The velocity between these levels was interpolated linearly. In our case, the Moho interface was presented as a high gradient level. For our study area the reference model was defined as in the table 2 (Kim and Gao, 1996; Kim and Gao,1997).

In such a presentation, Pg and Pn, Sg and Sn phases (refracted above and below the Moho) have not principal differences and they were considered together in the common inversion.

**Table 1.** Initial 1D velocity model.

Depth	V <sub>p</sub>	V <sub>s</sub>
-1.0	4.5	2.31
4.0	5.10	2.63
8.0	6.20	3.36
12.0	6.35	3.50
16.0	6.50	3.60
20.0	6.70	3.75
24.0	6.96	3.97
28.0	7.45	4.28
35.0	7.95	4.58
55.0	8.09	4.67
75.0	8.08	4.70
300.0	8.71	5.52

### Method of Event Location

All the data about North Korean seismicity were revised and the positions of hypocenters were recomputed anew. We used the algorithm to calculate the source position coordinates and origin times. This algorithm uses all rays available from the source recorded by the local

stations including P and S phases, rays in the crust and under Moho.

To compute the ray configurations and the reference travel times we used the analytical formulas of ray tracing in 1D medium with linear squared slowness. The change of velocity gradient in our reference model in some cases causes caustics at the travel time curve. In our algorithm we find all possible solutions for the rays between any two points, though we selected only the rays with amplitudes higher than a predefined minimal value. The amplitude was estimated as  $Amp = dx / da$ , where  $da$  is a small variation of the dipping angle,  $dx$  is corresponding variation of the epicentral distance.

To find the position of source we minimize the travel time least-squares error  $E = \sum_i^N (T_i^{obs} - T_i^{mod})^2 = F$ , where  $T_i^{obs}$  is travel time of  $i$ -th observation;  $T_i^{mod}$  is the corresponding travel time computed in the reference model,  $x, y, z$  are coordinates of the source;  $N$  is the number of recorded phases for one source; residual( $a_i$ ) means errors of  $a$ -vector values with respect to their average value. In the first step, to compute the observed travel times  $T_i^{obs}$

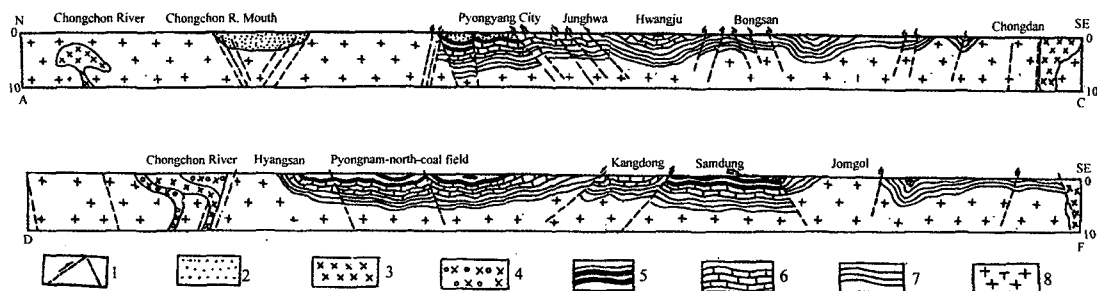


**Fig. 3.** Geological section of western Pyongnam Basin( Ro Su Won, 1964).

(ABC : Jongju-pyongyang-Chongdan, DEF : Chongchon River-Pyongnam north-Pyongnam south coal field Jomgol)

1. Thrust and reverse fault
2. Mesozoic and partial Cenozoic
3. Danchon rock
4. Hyesan rock
5. Pyongan system
6. Chosun system
7. Sangwon system(middle and upper Proterozoic)
8. Crystalline granite gneiss and crystalline schist

we use an arbitrary value of origin time (minimal arrival time among all observations) and  $\partial E / \partial x = \partial E / \partial y = \partial E / \partial z = 0$  for  $E$  to be minimized.

The method of determination of the source coordinates is illustrated schematically in Fig. 4. Contour lines show the value of the  $F$ -function. The minimal values are depicted with darker colors. In the first step, we find the approximate position of the source by analyzing the values of  $F$ -function in nodes of a regular grid. In reality, the shape of this function can be fairly complicated, and it can contain some false local minimums. To avoid a possibility of getting a wrong minimum, we find several best nodes (1-4, in Fig. 4). The precise location of the  $F$ -function minimum is computed starting from all these nodes using the gradient method. Light gray circles in Fig. 4 indicate the paths of searching; white circles are the final solutions. In case of nodes 1 and 4 we have false local

minimums. Only the paths from 2 and 3 nodes guide to the absolute minimum. After determining the minimum and calculating the travel times we compute the time residuals. If a residual for some phases is larger than 5 sec, this phase is rejected and all the aforesaid procedure is repeated again. The minimal number of phases recorded from one source was 10. The sources with lesser number of observations were rejected.

As the result, we have located 91 Korean earthquakes. Their distribution is shown in Fig. 2. Most of them are associated with the boundaries of different geological blocks and located on the main active faults. Average depth of Korean seismicity is about 15 km.

### Tomographic Inversion

Seismic tomography is one of the most

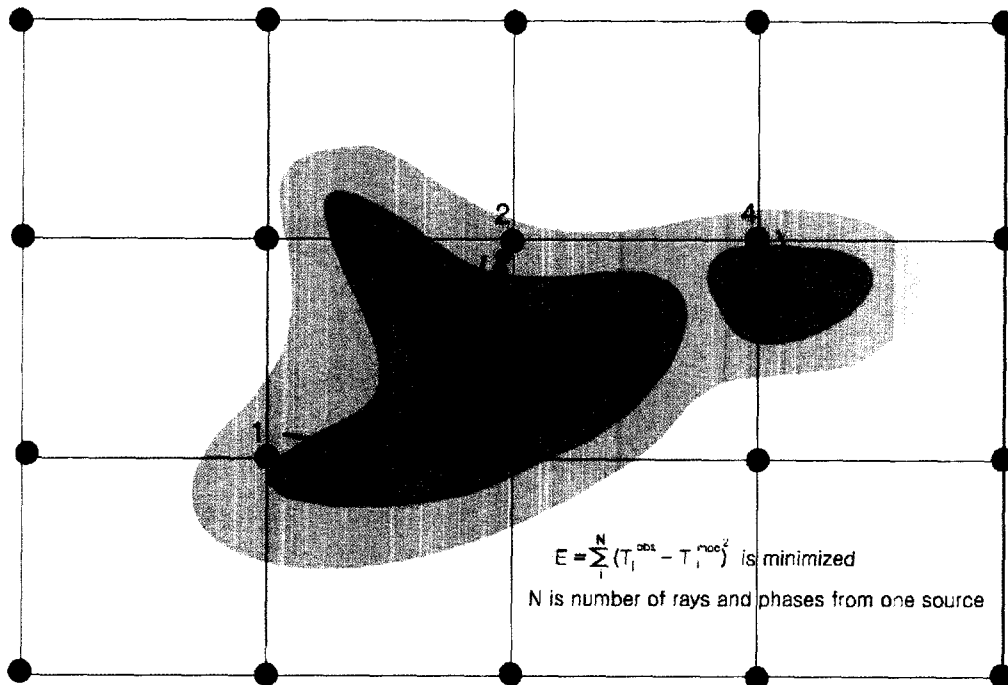


Fig. 4. Finding of the seismic source localization

important methods to investigate the deep structure of the earth. Thanks to seismic tomography, reliable and high resolution models have been obtained in many regions of the earth. The global model of the mantle (Bijwaard et al., 1998) provides structures which in most cases has a clear interpretation and is consistent with other results obtained at regional scales. Though, the paradoxical situation is that the crustal structure in most regions is known much less than the global mantle structure. To study the crust, both developed seismic networks and sufficiently high seismicity must take place, while in the deep mantle a good intersection system under some regions can be obtained due to the intersection of teleseismic rays from different regions. Another method for crustal investigation, deep seismic sounding (DSS), provides much more reliable results than seismic tomography, since it is based on powerful artificial explosions with known origin times and coordinates. However, utilization of DSS is usually limited due to the very high expenses of the experiments and ecological danger. That is why, seismic tomography based on natural sources, earthquakes, is still one of the most important tools to get information about seismic structure in the crust. There are some successful examples of the realization of the local scheme in different parts of the world (e.g. Roecker, 1993; Petit et al., 1998).

We used a technique of parameterization and tomographic inversion, which was applied for the teleseismic approaches (Koulakov, 1998; Koulakov et al., 1995). Now it is transformed for the local tomography purposes. As a parameterization, we use the grid which is constructed according to the ray density. The nodes of the grid are installed on a certain number of the depth levels. To construct this grid we compute the 3D function of density of the real rays traced in the reference model. The nodes are equally installed in every layer so that

the total length of the rays around every node was approximately equal. The examples of the ray density plots and the position of nodes at different depth levels are shown in Fig. 8. After this step, the study volume is subdivided into the tetrahedral blocks with vertices coinciding with nodes of the grid. Inside every block we define a constant velocity gradient that provides the continuous velocity distribution in the study volume. The method of non-uniform parameterization allows more uniform filling of the first derivative matrix that leads to a higher stability of the inversion.

Our technique of the grid construction requires an initial orientation that has a certain influence upon the nodes position since the densities of ray path are dependent on the grid orientation. Correspondingly, the result of inversion depends slightly on the orientation of the grid. To avoid this, for the same region we have made several inversions with different initial orientations of the grid. The influence of grid orientation for the case of the Korean data is considered in one of the tests in Fig. 10 (influence of the grid orientation),

The first derivative matrix of  $dV_i / dT_j$  (influence of velocity variation in  $i$ -th node upon the travel time of  $j$ -th ray) is computed on the basis of the rays traced in the reference model. For every point of the ray we determine the number of the tetrahedron in which it is located and four nodes which have an influence on it. Denote the elementary segment of the  $i$ -th ray as  $dS$ . The elementary delay at this segment is due to the velocity variation at the  $j$ -th node, and is computed as:

$$dt_i = - \Delta V_j (S) dS / V^2$$

where  $V$  is the average velocity in a point of the ray,  $\Delta V_j$  is the velocity variation in the point of the ray related to the elementary

velocity variation in the  $j$ -th node. The influence of each node is integrated along the  $i$ -th ray and divided by the velocity variation in the  $j$ -th node. The integration along the ray path gives the  $A_{ij}$  element of the first derivative matrix. The obtained matrix has the number of columns equal to the number of parameters and number of rows equal to number of rays. This matrix is rare, and all non-zero elements are negative. The columns and rows of the matrix are filled approximately uniformly due to the special way of parameterization. That is very favorable for the inversion stability. The LSQR method was used to make the inversion of the matrix (Paige and Saunders, 1982; van der Sluis and van der

Vorst, 1987).

The final results are computed as a summary of the four models with differently orientated grids. The obtained 3D structure is presented in Fig. 5, 6 and 7. Fig. 5 shows horizontal sections of P-wave velocity anomalies at four depth levels. Blue colors depict high velocity anomalies. Blank areas mean the places where the distance to the nearest node is larger than 50 km. Horizontal sections of S-wave velocity anomalies are shown in Fig. 6. We present also two vertical sections for P and S models on Fig. 7. The position of the sections is shown on the map on the left side of the figure. The velocity anomalies are obtained at four depth

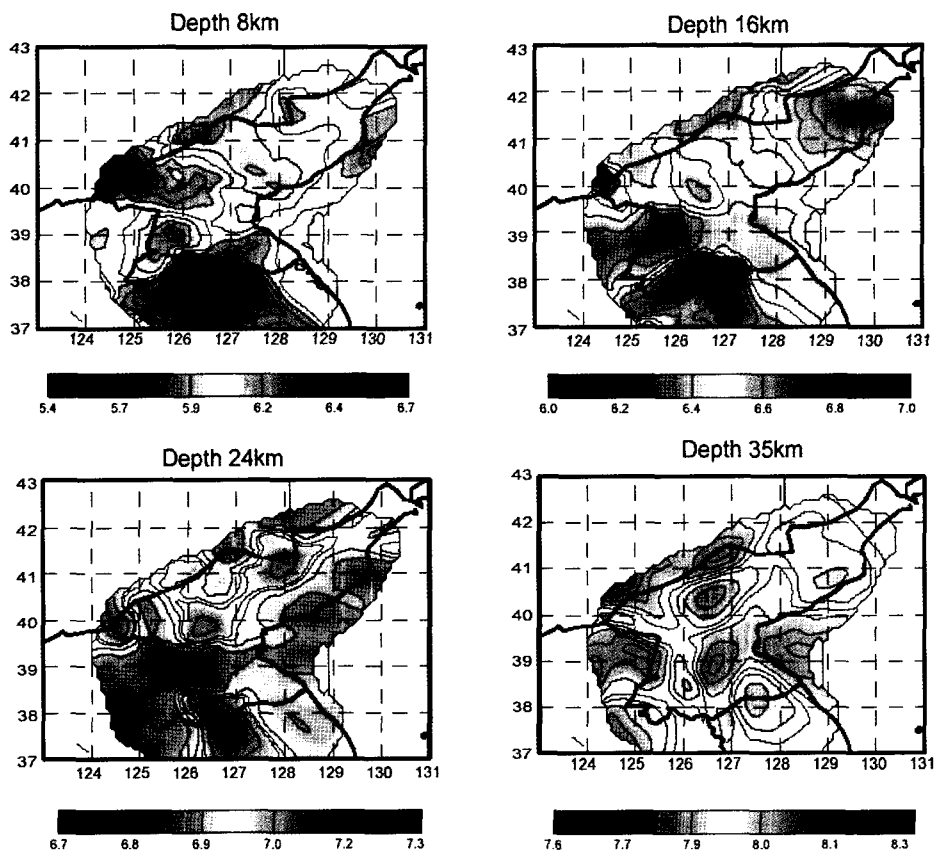


**Fig. 5.** P-wave velocity anomalies for horizontal sections at different depth levels. Blue shades indicate high velocity.



3차원 속도 토모그래피를 이용한 북한지역의 지각구조 연구

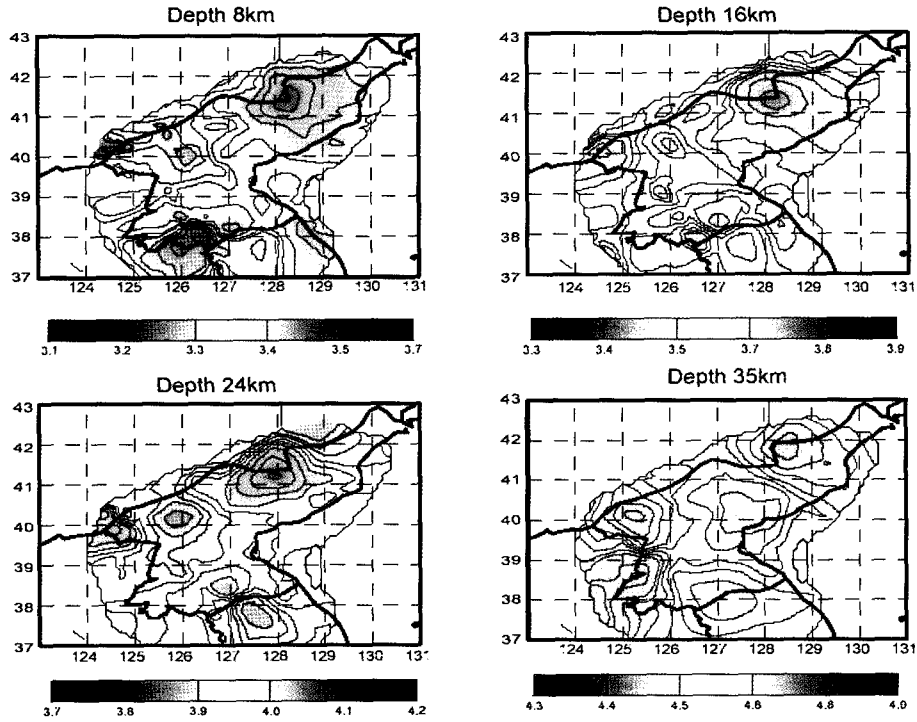


**Fig. 6.** S-wave velocity anomaly for the horizontal sections at different depth levels. Blue shades indicate high velocity.

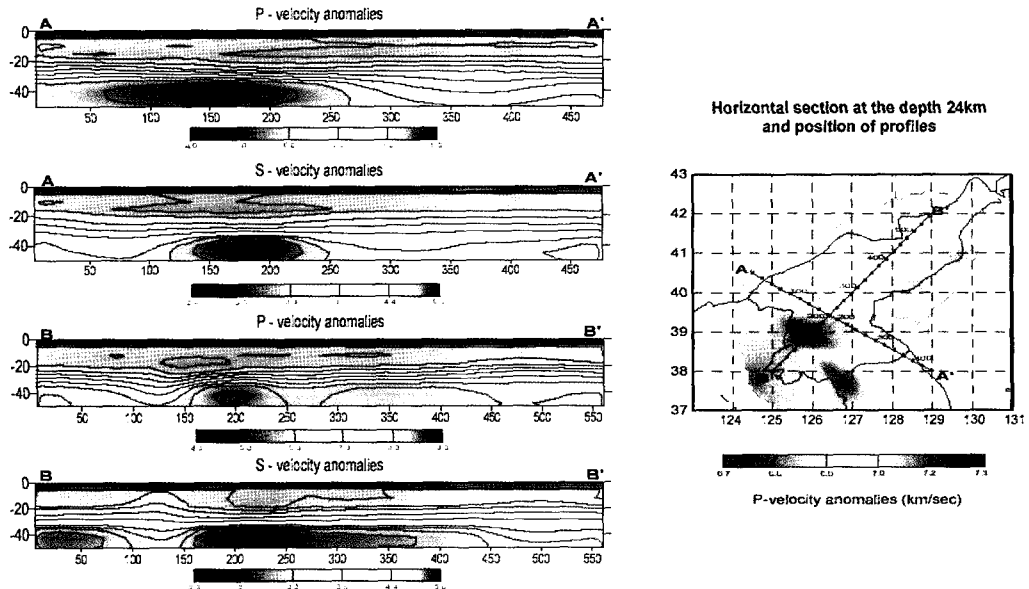


**Fig. 7.** Vertical sections of P- and S-wave velocity anomalies along two lines in North Korea. Blue colors indicate high velocity.

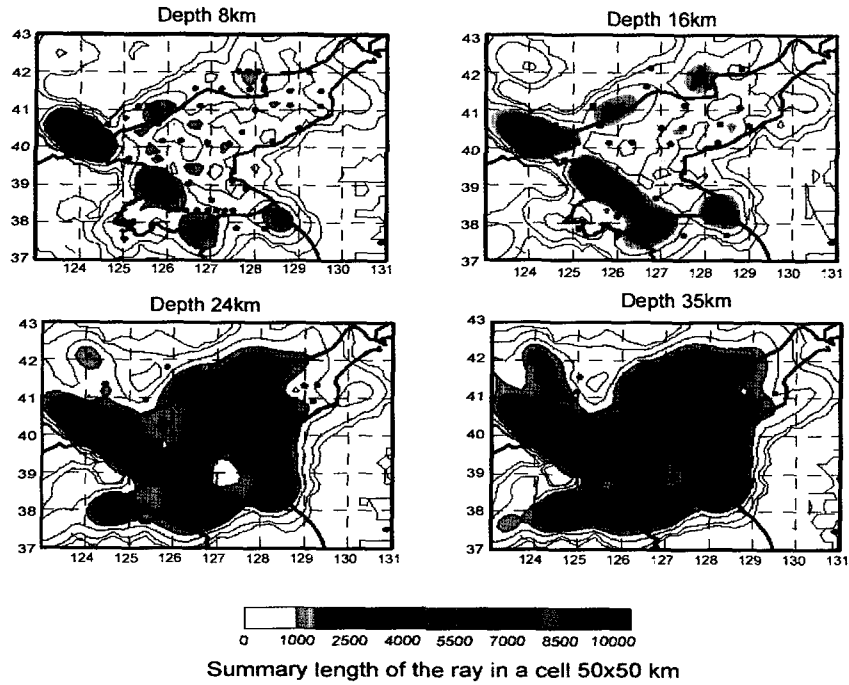


**Fig. 8.** Plots of the ray density at different depth levels and distribution of the parameterization nodes.

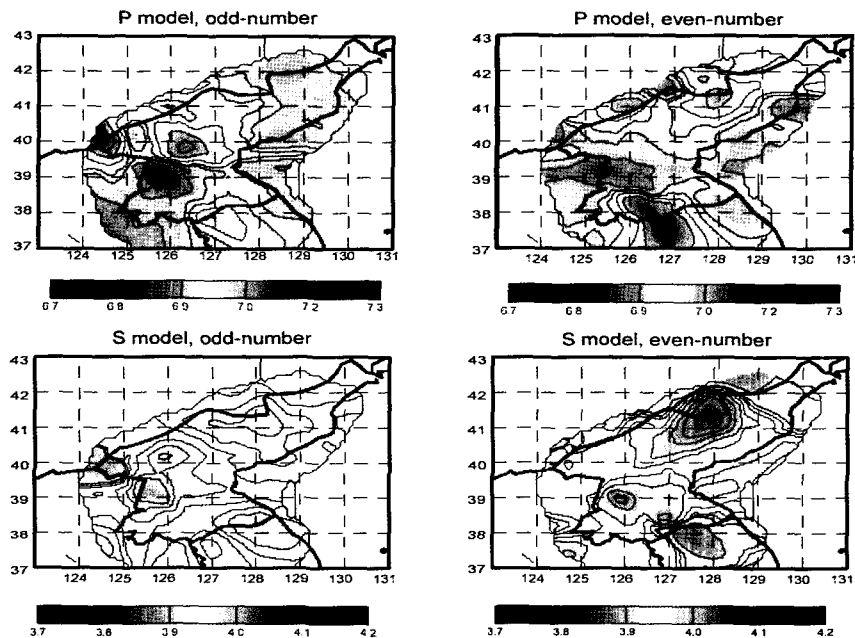


**Fig. 9.** Test with inversion of different datasets for odd-number and even-number earthquakes at 24 km of depth.

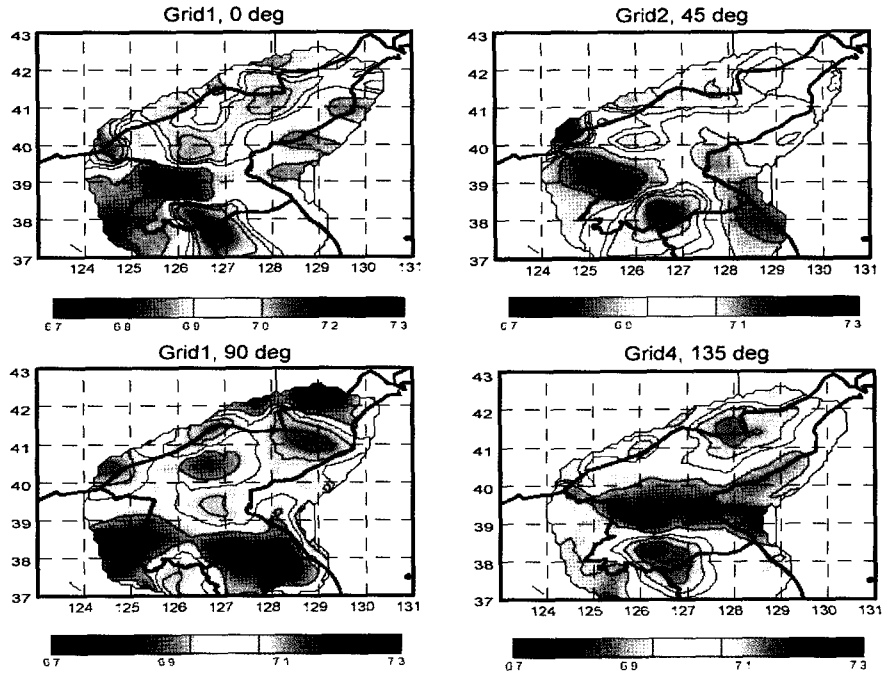


**Fig. 10.** Test with inversion using differently oriented grids. Here is an example of P-wave model of 24 km.

levels. Velocity distribution between these levels is interpolated linearly. Before giving the interpretation of these results, let us present some tests which illustrate the reliability of the obtained anomalies.

As we mentioned above, construction of the parameterization grid in our algorithm needs some initial orientation. Different values of this parameter cause a slight variation of the nodes position. Comparison of the results obtained for different grids and their summation helps us to see the artifacts related to the grid orientation and to extract the anomalies which are common in all cases. An example of this test is shown in Fig. 10. Here we present the horizontal sections of P-wave velocity anomalies at a depth of 24 km, obtained with four grids of different initial orientation. As we can see, there are some small anomalies which can be considered as artifacts. But the main high

velocity anomalies larger than 50 km are observed in all plots and have approximately the same shape.

In the second test, data were arbitrarily divided into two equal groups and earthquakes were assigned odd and even numbers. The results of independent inversion with these datasets are shown in Fig. 9. Comparison of these maps gives an idea about reliability of anomalies and their independence from the random effects. This test shows that all anomalies larger than 50 km are reconstructed in both maps and they can be considered as valuable.

## Geological Interpretation

New results about the crustal structure down to a depth of 60 km beneath North Korea were

obtained using the seismic tomography method. About 1013 P- and S-wave travel times from local earthquakes and explosions recorded by the Korean stations and the vicinity were used in the research. Parameterization of the velocity structure is realized with a set of nodes distributed in the study volume according to the ray density. 120 nodes located at four depth levels were used to obtain the resulting P- and S-wave velocity structures. In order to construct the tetrahedral blocks, we subdivide the triangulate prisms into tetrahedra using the neighboring nodes of upper and lower levels.

As a result, it is found that P- and S-wave velocity anomalies of the Rangnim Massif at depth of 8 km are high and low, respectively, whereas those of the Pyongnam Basin are both low up to 24 km. It indicates that the Rangnim Massif contains Archean-early Lower Proterozoic Massif foldings with many faults and fractures which may be saturated with underground water and/or hot springs. On the other hand, the Pyongyang-Sariwon in the Pyongnam Basin is an intraplateau depression which was filled with sediments for the motion of the Upper Proterozoic, Silurian and Upper Paleozoic, and Lower Mesozoic origin. In particular, the high P- and S-wave velocity anomalies are observed at depth of 8, 16, and 24 km beneath Mt. Backdu, indicating that they may be the shallow conduits of the solidified magma bodies, while the low P- and S-wave velocity anomalies at depth of 38 km must be related with the magma chamber of low velocity bodies with partial melting. We also found the Moho discontinuities beneath the Ongjin Basin including Sariwon to be about 55 km deep, whereas those of Mt. Backdu are found to be about 38 km (Lee, 1997). The high ratio of P-wave velocity/S-wave velocity at Moho suggests that there must be a partial melting body near the boundary of the crust and

mantle. Consequently, we may well consider Mt. Backdu as a dormant volcano which is holding the intermediate magma chamber near the Moho discontinuity. This study is consistent with North Korean study of Mt. Backdu (Yoon, 1993).

This study also brought interesting and important findings that there exist some materials with very high P- and S-wave velocity anomalies at depth of about 40 km near Mt. Myohyang area at the edge of the Rangnim Massif shield. It may be related to the very high density of ultramafic rock containing kimberlite type in the Archean basement. This is proved by finding the Archean intrusive ultramafic rocks of the Andol Complex around this region. It is also reported that some kimberlites without diamond have been found in Bakchon-Kisongri areas. Taking into account the crust-mantle deep faults running from Sakju to Wonsan in NW-SE, it is evident that there were some large tectonic movements across the Pyongnam North Coal Field near the boundary between Rangnim Massif and Pyongnam Basin. Therefore, we cannot refuse to say that there are some potential deposits of diamond in the Liadong-North Korea Shield Platform (Kharkiv et al., 1997).

## Conclusion

The seismic tomography of North Korea has not been revealed as compared to the central and southern Korean Peninsula. The object of this research is to determine the crustal structure of North Korea using local tomography. This study, however, is the only preliminary result due to lack of data and poverty of information. This work will be improved provided more data and information are obtained.

1) The high P- and low S-wave velocity anomalies at the depth of 8 km indicates that the Rangnim Massif contains Archean-early Lower Proterozoic Massif foldings with many faults and fractures that are saturated in ground water and/ or hot springs.

2) The low P-and S-wave velocity anomalies up to 24 km deep indicates that the Pyongnam Basin consists of an intraplatform depression which was filled with sediments for the motion of the Upper Proterozoic, Silurian and Upper Paleozoic, and Lower Mesozoic origin.

3) The high P-and S-wave velocity anomalies at depth of 8, 16, 24 km beneath Mt. Backdu depict the shallow conduits of the solidified magma bodies, while the low P-and S-wave velocity anomalies at the depth of 38 km suggest the magma chamber of low velocity bodies with partial melting.

4) We found the Moho discontinuities beneath the Ongjin Basin including Sariwon to be about 55 km with subsidence, whereas beneath Mt. Backdu, the Moho discontinuity is found to be about 38 km with high ratio of P-wave velocity/S-wave velocity at this depth, indicating that there must be a partial melting body at the boundary between the crust and mantle. We may well consider Mt. Backdu as a dormant volcano, which is holding the intermediate magma chamber at Moho discontinuity.

5) Finally we found very interesting and important bodies that have very high P-and S-wave velocity anomalies at depth of about 40 km near Mt. Myohyang area of the edge of the Rangnim Massif Shield. They may be related to the high density ultramafic rock containing some kimberlites in the Archean basement. Taking into account the Archean intrusive ultramafic rocks of the Andol Complex and deep faults of crust-mantle, one cannot rule out the possibility of some potential deposits of

diamond in the Liadong-North Korea Shield Platform.

This study is a preliminary important step for investigating the complex crustal structure of the Korean peninsula. The results obtained in this research seem to be stable and reliable, and their apparent correlation with other geological and geophysical observations gives rich material for understanding the deep processes in the Korean peninsula.

## Acknowledgments

This work is supported by KMA (Korea Meteorological Administration) under Korea Ministry of Science and Technology. We appreciate the support of the program by Koulakov.

## References

- Mt.Backdu series (Geology), 1993, Ed. Yoon Bok Dong, Science and Technology Publisher, Pyongyang, DPRK, p. 367
- Bijwaard, H, W.Spakman, and E.R.Engdahl,1998, Closing gap between regional and global travel time tomography, J. Geophys. Res., 103, 30055-30078.
- Choi, K. S., G.V.R. Kumar, and K. Y. Kim,1999, Qualitative interpretation of Bouguer anomaly in the southern part of the Korean Peninsula, Geoscience Journal, v. 3, n. 1, p. 49-54.
- Geology of Korea ,1987, Ed. D.S.Lee, The Kyohak-Sa Publishing Co., Seoul, Korea, 514p.
- Gology of Korea ,1993, Foreign Language Book Publishing House, Pyongyang, DPRK, 619p.
- Geological Structure and Underground Resources of NE Chosun and the maritime province

- south of Siberia, 1964, Institute of Geology and Geography, Academy of Sciences, DPRK and Institute of Geology, Vladivostok, Siberian Branch, Academy of Sciences, USSR. 472p.
- Kharkiv, A. D., N. N. Zinchuk and B. M. Zuev, 1997, *Diamond History*, Nedra, Moscow, 601p.
- Kim, So Gu, Erdenedalai Lkhasuren and Pil-Ho Park, 2003, The low seismic activity of the Korean Peninsula surrounded by high earthquake countries, *Journal of Seismology*(in press).
- Kim, S. G. and F. Gao, 1996, Seismic investigation in the central Korean Peninsula using the artificial chemical explosions, *Bulletin of the Seismological association of the Far East(BSAFE)*, v. 2, n. 1, p. 18-46.
- Kim S. G. and F. Gao, 1997, Preliminary Crustal Studies of the Korean Peninsula Using Lg-coda Q, *Bulletin of the Seismological Association of the Far East*, v. 3, n. 1, p. 121-139.
- Kim S. G. and S. K. Lee, 1997, Determination of the crustal structure beneath the Korean seismic stations using receiver functions, *Bulletin of the Seismological Association of the Far East*, v. 3, n. 1, p. 45-59.
- Kim, S. G. and Q. Li, 1998a, 3D crustal velocity tomography in the southern part of the Korean peninsula, *Econ. Environ. Geol.*, v. 31, n. 2, p. 127-139.
- Kim, S. G. and Q. Li, 1998b, 3D crustal velocity tomography in the Central Korean peninsula, *Econ. Environ. Geol.*, v. 31, n. 3, p. 235-247.
- Kim, S. G., Q. Li, E. Lkhasuren, J. Lee, and H. S. Jang, 2000, 3D seismic tomography using traveltimes and waveform of melt-phase, *CT Theory and applications*, v. 9, n. 4, p. 44-47.
- Kim, S. G. and E. Lkhasuren, 2000, Why is the Korean Seismicity not so severe as the vicinities such as NE China, SW Japan, and Sakhalin? *Bulletin of the Seismological Association of the Far East*, Vol. 4, No. 1, 107-114.
- Kim, S. G. and J. Song, 1999, Stress field study in the vicinity of the Korean Peninsula using shear-wave splitting, *Jour. Korean Earth Science Soc.*, v. 20, n. 2, p. 166-178.
- Koulakov I. Yu., 1998, 3D tomographic structure of the upper mantle beneath the central part of Eurasian continent, *Geophys. Journ. Int.*, 1998, v. 133, n. 2, p. 467-489.
- Kulakov, I. Yu., Tychkov, S. A. and Keselman, S. I., 1995, Three-dimensional structure of lateral heterogeneities in P velocities in the upper mantle of the southern margin of Siberia and its preliminary geodynamic interpretation. *Tectonophysics*, 241: 239-257.
- Lee, S. K. , 1997, Study on the crustal structure of the Korean Peninsula using receiver function and seismic tomography, Ph. D. thesis, Hanyang University, 248p.
- Paige, C. C., and M. A. Saunders, 1982, LSQR: An algorithm for sparse linear equations and sparse least squares, *ACM trans. Math. Soft.*, v. 8, p. 43-71.
- Petit C., Koulakov I., Deverchere, J., 1988, Velocity structure around the Baikal rift from teleseismic and local earthquake traveltimes and geodynamic implications, *Tectonophysics*, v. 296, p. 125-144.
- Roecker, S. W., 1993, Tomography in zones of collision: Practical considerations and examples, in *Seismic tomography, theory and practice*, edited by H.M.Iyer and K.Hirahara, pp. 584-612, Chapman and Hall, London.
- Shin, Jong Woo, 2003, Crustal Structure of North Korea Using Seismic Tomography, M.S. Thesis, Hanyang University, 133p.
- Van der Sluis, A., and H. A. van der Vorst, 1987, Numerical solution of large, sparse linear

3차원 속도 토모그래피를 이용한 북한지역의 지각구조 연구

algebraic systems arising from tomographic problems, in: Seismic tomography, edited by G.Nolet, p. 49-83, Reidel, Dordrecht.

투 고 일	2003년 6월 30일
심 사 일	2003년 7월 1일
심사완료일	2003년 7월 28일

---

김소구  
한양대학교 지구해양과학과  
426-791경기 안산시 상록구 사1동  
Tel: 031-400-5532  
Fax: 031-400-5532  
E-mail: sogukim@hanmail.net

신종우  
국립문화재연구소 유적조사연구실  
110-050 서울시 종로구 세종로 1-57번지  
Tel: 016-336-9851